SUPPORTING INFORMATION

Selective microwave sensors exploiting the interaction of analytes with trap states in TiO$_2$ nanotube arrays

M. H. Zarifi,[1] S. Farsinezhad,[1] M. Abdolrazzaghi,[1] M. Daneshmand[1] and K. Shankar[1, 2]

[1]Department of Electrical and Computer Engineering, University of Alberta, 9107 - 116 St, Edmonton, Alberta, Canada T6G2 V4

[2]NRC National Institute for Nanotechnology, 11421 Saskatchewan Dr NW, Edmonton, AB T6G 2M9

Section S1: Materials and Methods

Microwave resonator sensor fabrication and measurement setup

The planar microwave ring resonator was implemented on a microwave substrate from Rogers Corporation (5880). The substrate has a relative permittivity of 2.2 with a loss factor of 0.0009 and thickness of the dielectric material of 0.79 mm. Metallic copper with a thickness of 35 μm and conductivity of 5.8 MS/m covers both sides of the substrate. Wet chemical etching printed circuit board (PCB) development technique was performed to implement the ring resonator. The fabricated resonator was directly connected to a vector network analyzer (ZVL 13, Rohde and Schwartz) for S-parameter measurements. ANSYS HFSS was use to perform all electromagnetic simulations. All the experiments were performed at 21 °C at a relative humidity of 21 %. An Omega temperature and humidity sensor was used to continuously monitor these parameters. The flow rates were kept constant at 500 SCCM using MFC (mass flow controllers) from Alicat Company. The TiO$_2$ nanotube membrane layer was placed on the top surface of the microwave resonator without any adhesive layer. Before every experiment, the PCB surface was cleaned with IPA and dry air was purged to the chamber for 10 min. The chamber was a plastic container $11 \times 8 \times 6 \ \text{cm}^3$ with sealed electric and gas feeding throughputs.

Dimensions of the ring resonator

W= 1mm

g= 1mm

Nanotube membrane preparation

Prior to the anodization, titanium sheets approximately 0.89 mm thick (99.9% purity; Alfa Aesar) with sizes of about 1 cm x 4 cm and 0.5 cm x 4 cm were utilized as anode and cathode respectively. These substrates were ultrasonically cleaned in acetone (99.5%, from Fisher Scientific), methanol (99.8%, from Fisher Scientific), and water for 10 minutes each, followed by rinsing in deionized water and blow drying with Nitrogen gas. The electrochemical anodization process of the titanium was carried out at room temperature in a two-electrode electrochemical cell by using a direct current source at a constant voltage of 60 V for 72 hours. The anodization process was performed in an electrolyte containing 4% deionized water, 0.3 wt% ammonium fluoride (98.3% from Fisher Scientific) and rest ethylene glycol (99.9%% from Fisher Scientific). In order to achieve self-standing membranes, the TiO_2 nanotube layer was detached from the Ti sheet surface by rinsing the substrate with water and methanol right after anodization. In this case, the as-prepared self-standing TiO_2 nanotubes are amorphous. The thermal annealing was conducted at around 360 °C in air for 16 hours to induce crystallinity.

Nanotube Membrane Characterization Techniques

The morphologies of the TiO_2 nanotube membranes were examined using a field emission scanning electron microscope (Zeiss Sigma) operating at 5 kV accelerating voltage by secondary electron imaging. The internal structure of samples were imaged using high resolution transmission electron microscopy (HRTEM) (JEOL 2200FS) operating at 200 kV, equipped with scanning transmission electron

microscopy (STEM) and energy dispersive x-ray facility. TEM sample preparation of the nanotube cross sections was performed using focused ion beam etching in a SEM system (Hitachi-NB5000). Fourier Transform Infrared Spectroscopy (FTIR) was performed using a Varian FTS-7000 instrument. The high equilibrium carrier concentration and photon scattering in the nanotube membrane made it impossible to derive useful signal in transmittance or in infrared reflection absorption spectroscopy (IRRAS) modes; instead, Attenuated Total Refelectance (ATR) mode was found to provide the best signal to noise ratio.

Characterizing complex permittivity and obtaining the nanotube microwave spectral behavior

Wide frequency band behavior of nanotubes was characterized using the dielectric probe kit Model no. DPS16 from Keycom Characteristic Technologies connected to a ZVA67 Rohde & Schwartz VNA. The data was saved during the time while the nanotubes were illuminated and also during the relaxation time. The results are presented in Figure S4 and Figure S5.
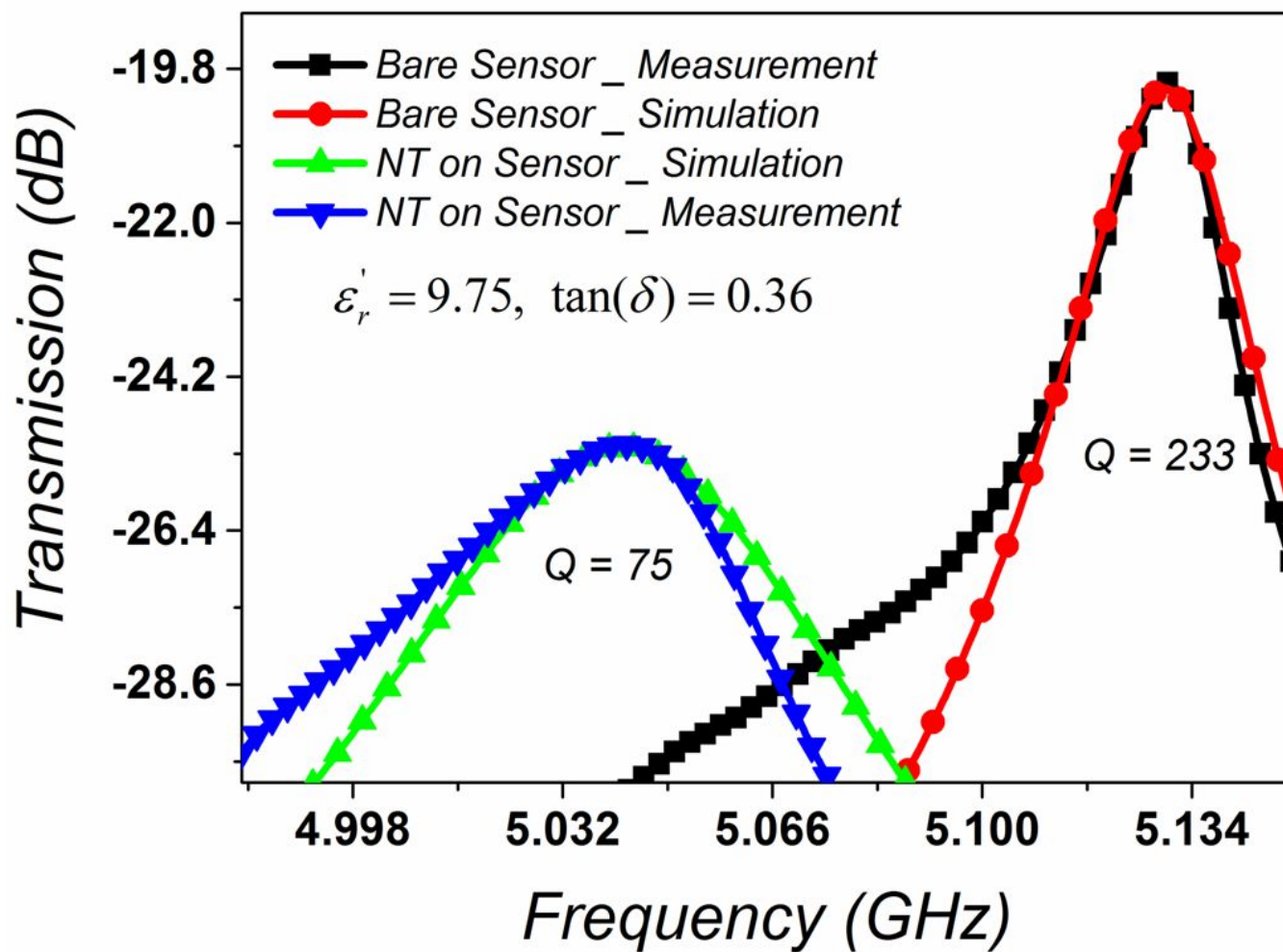
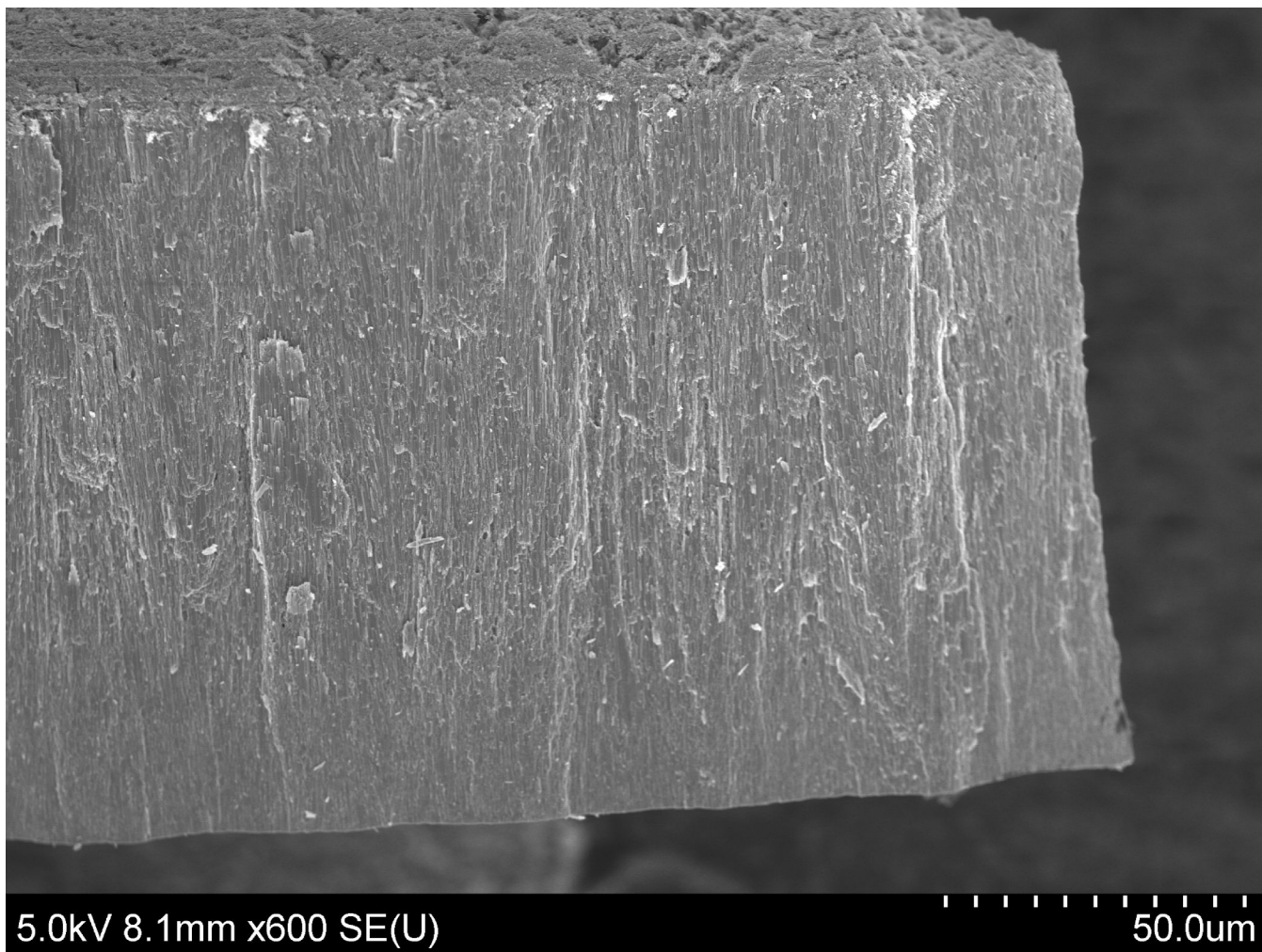**Figure S1.** Cross-sectional FESEM image showing the entire thickness of the TiO$_2$ nanotube membrane

5.0kV 8.1mm x600 SE(U)   50.0um

Figure S2. Cross-sectional FESEM image showing the entire thickness of the TiO_2 nanotube membrane
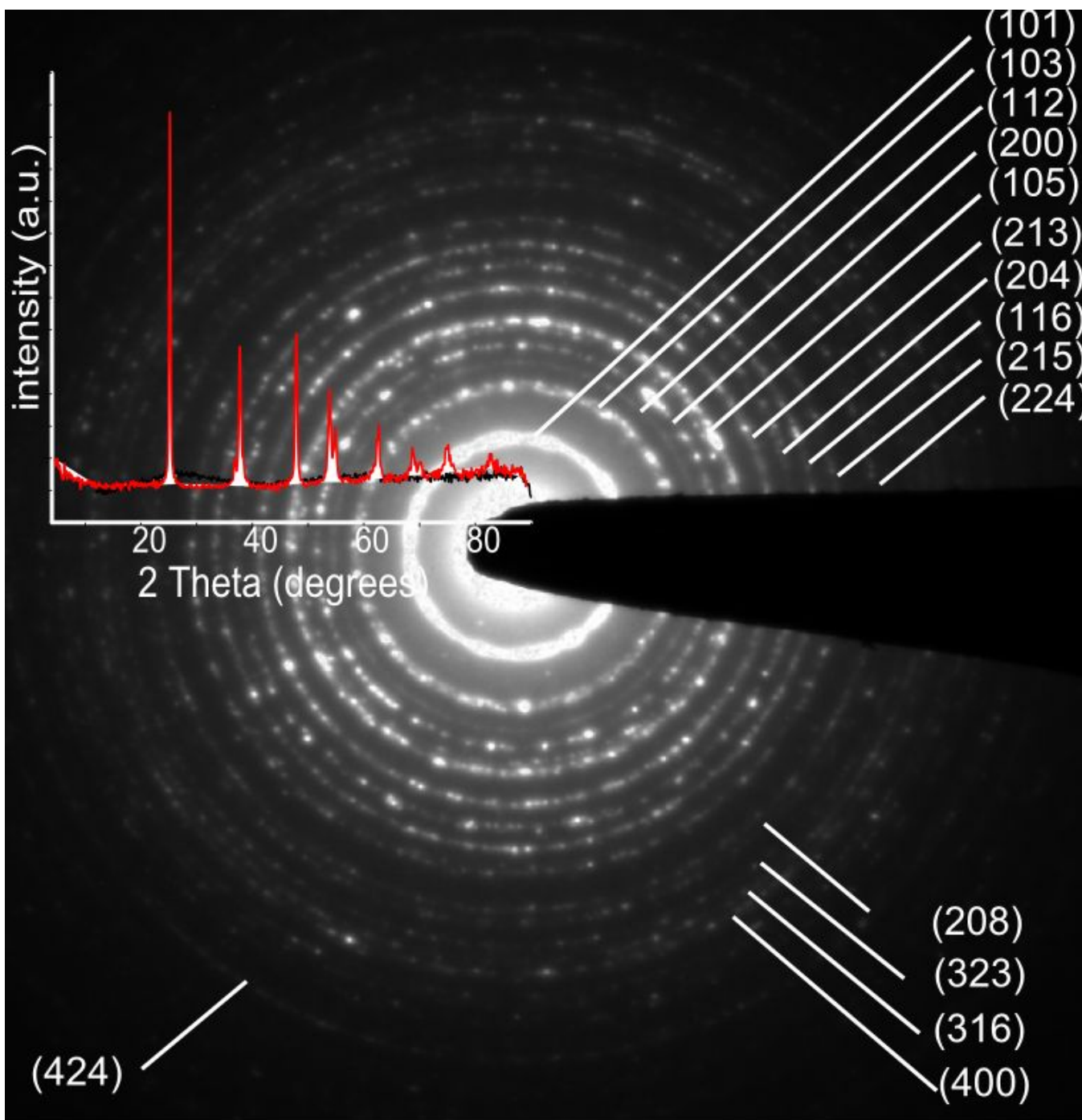
Figure S3. Electron diffraction pattern obtained from the TiO$_2$ nanotube membrane samples indicating good crystallinity and the presence of the anatase phase. The concentric rings which correspond to different crystal planes observed in polycrystalline TiO$_2$ nanotubes, are used to sequentially generate the diffractogram shown in the inset (red curve).
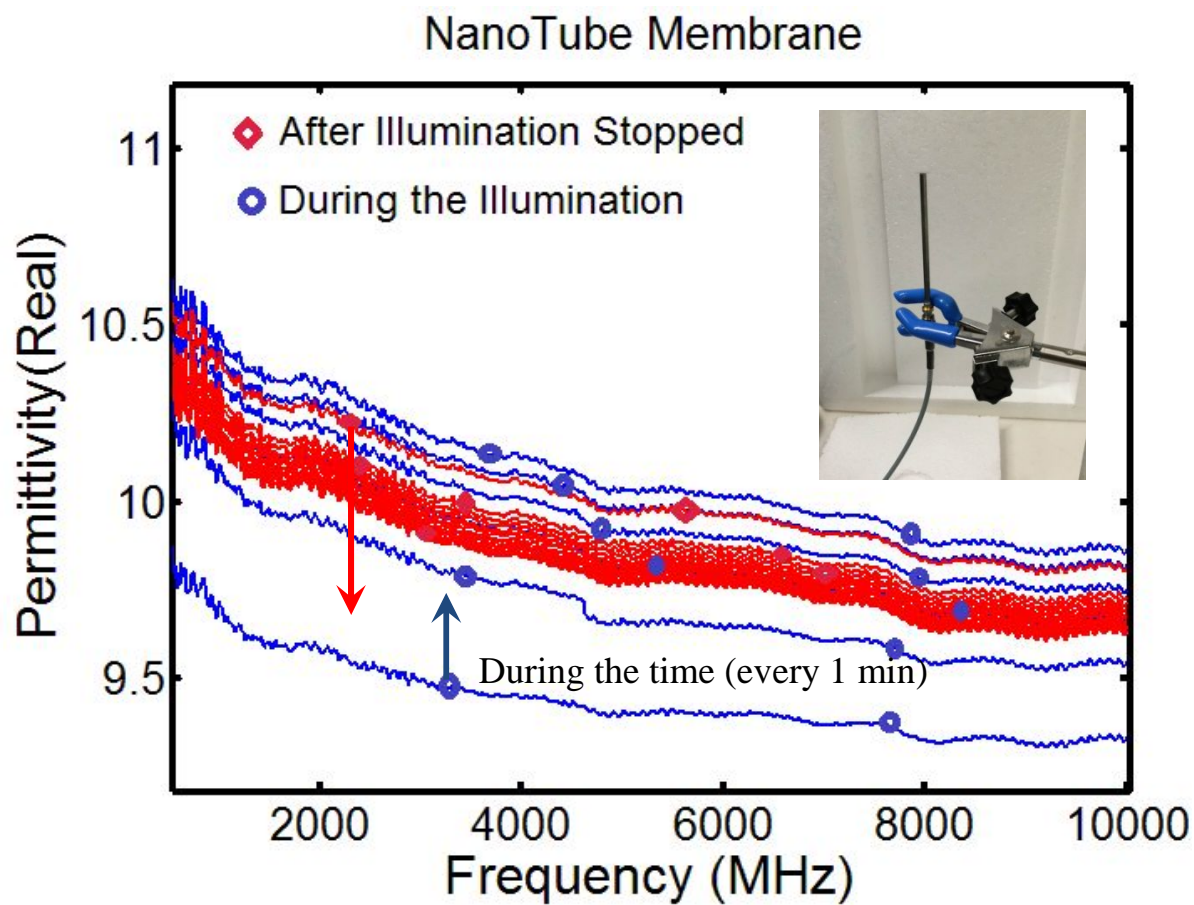
Figure S4. Dielectric permittivity spectra obtained from the TiO$_2$ nanotube membrane samples before, during and after illumination from a 254 nm lamp, using the dielectric probe.
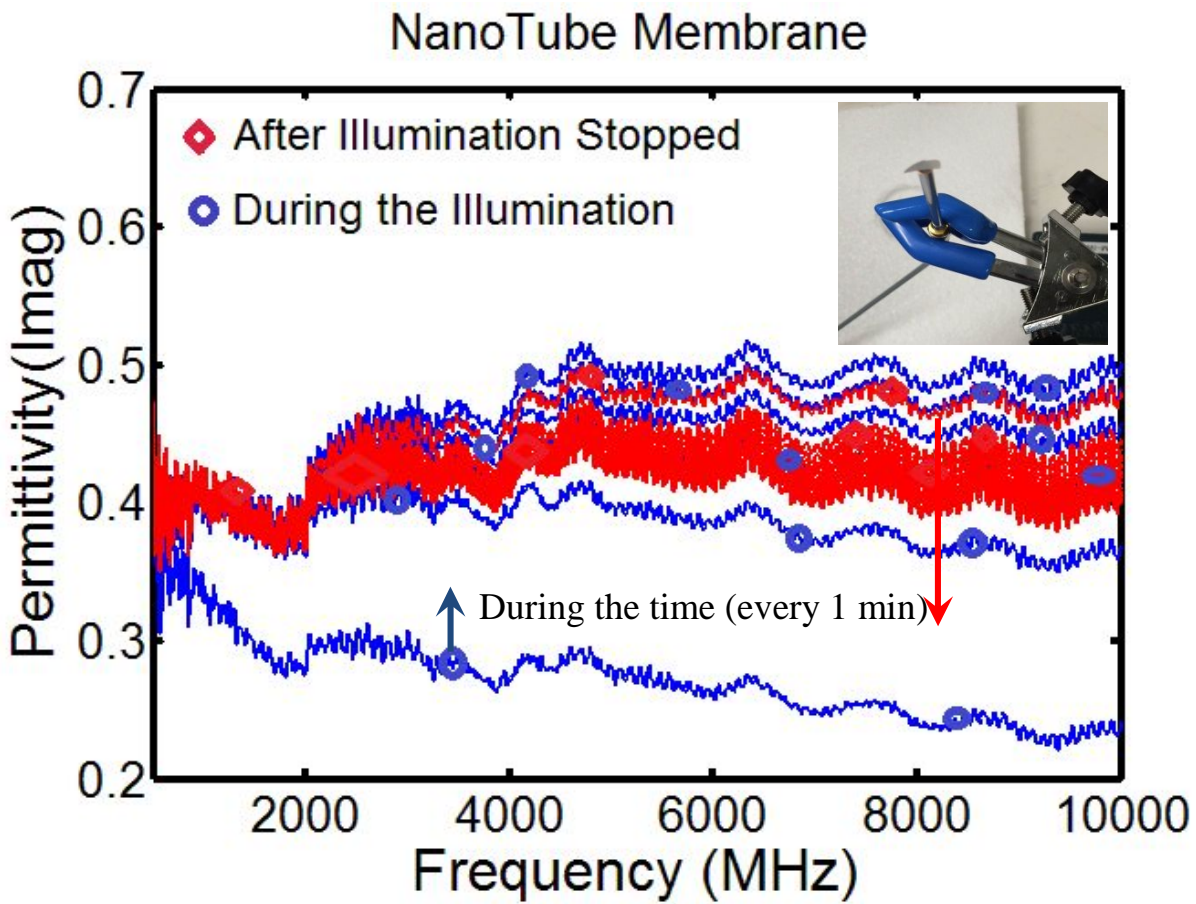
Figure S5. Dielectric loss spectra obtained from the TiO$_2$ nanotube membrane samples before, during and after illumination from a 254 nm lamp, using the dielectric probe.

Section S2: Extraction of additional electrical parameters in microwave resonator-based sensing

The variation of the f_0 and Q decays with concentration for each individual species is additional information not obtainable in a standard resistive sensor. Furthermore, deeper analysis of the microwave circuit allows one to extract a range of electrical parameters that change as a function of chemical species, illumination level and concentration as explained below. Based on the following equivalent circuit for the system, the open ended resonator has been simulated with a parallel RLC circuit which is coupled to the transmission lines with series capacitance and resistors. Here the principal resonance comes from a parallel RLC circuit which is highly dependent on the couplings as the equivalence of their mutual effects would result in the changes in resonance frequency (f_r representing the frequency at which maximum power transmission is happening), amplitude (T representing the amount of transmission at resonance) and quality factor (Q representing the sharpness of the profile). These 3 factors are independent of each other which is a key factor that helps us gather more information out of any single transmission profile. In other words, f_r deals with only one frequency at which a peak occurs, T reveals the relative power being transmitted at f_r, and Q interacts with both frequencies and amplitude, thus, have information about both the frequencies and amplitude at the same time.
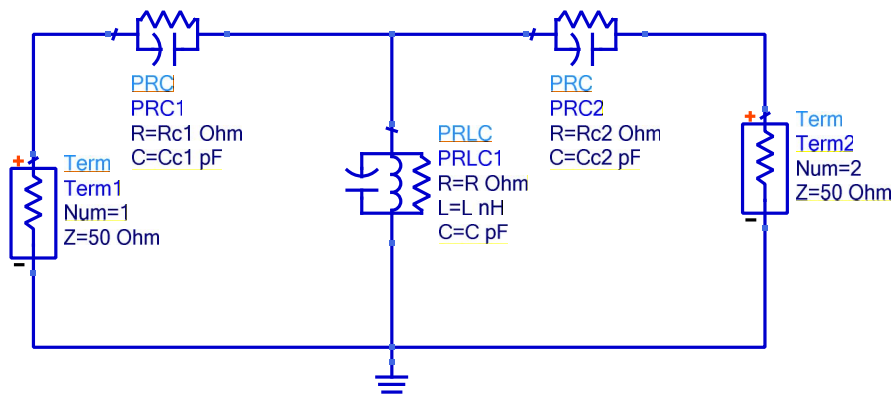

Figure S6. RLC circuit used to model the microwave resonator

In order to show the effect of each parameter in the profiles, 3 distinctive behaviors of the sensor during the experiment have been chosen and their equivalent circuits extracted in ADS as follows (here the word shining is used interchangeably with the word illumination):
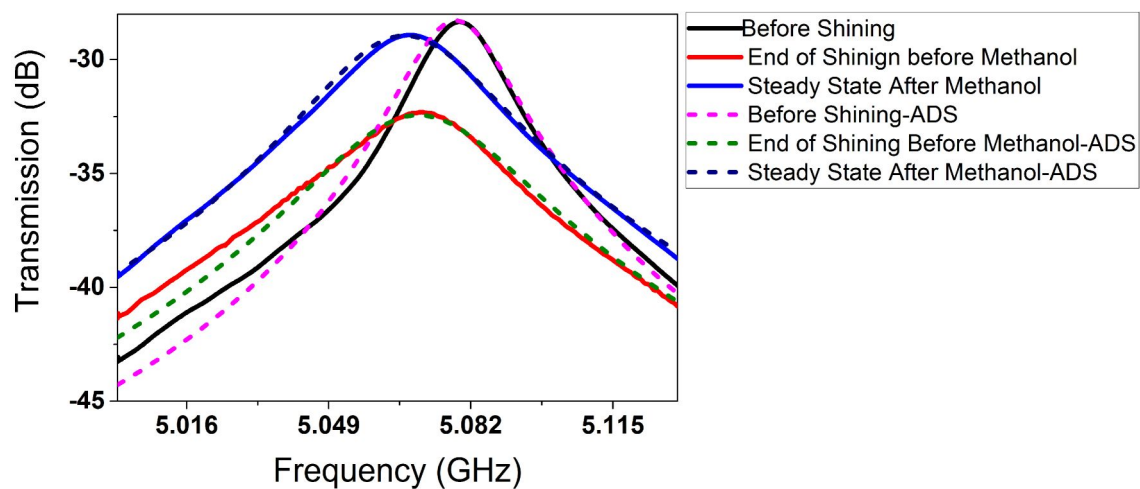

Figure S7. Resonance profiles obtained during experiments for different sensor states and fitted to simulations in ADS using the model in Figure S6.

Component	R (Ohm)	L (nH)	C (pF)	Rc1 (kOhm)	Rc2 (kOhm)	Cc1 (pF)	Cc2 (pF)
Before Shining	90	0.013	73.54	2.000	10	0.045	0.1
End of Shining Before Methanol Injection	55	0.013	73.54	1.145	10	0.317	0.1
Steady State After Methanol Injection	100	0.013	73.54	3.150	10	0.340	0.1

Table S1. The values for each component in Figure S6 corresponding to different sensor states

Here Rc1 and Cc1 have major effects while the resistance of the resonator is affected by the introduction of external material as well. The changes in 3 states, namely **A) Before Shining**, **B) End of shining before Methanol injection** and **C) Steady State after Methanol injection** are stated. Ultraviolet illumination of the nanotubes produces excess carriers and fills trap states, and these bound charges in turn increase the coupling capacitance (Cc1) while the coupling and internal resistances decrease (because of the higher carrier concentration) which is schematically depicted in the **Figure S6**. In state C, where the hole- scavenging effect due to the introduction of methanol causes the reverse phenomenon as the capacitance increases slightly (due to the increase in environmental permittivity in comparison to air) but the number of carriers is reduced due to the hole scavenging effect of methanol, therefore, the resistance increases. As a result, the main characteristics that are being used in order to recognize the vapors, are contained in 3 different classes of information as $f_r, Q \, and \, T$, each of them have distinctive meaning supporting the profile. The final role of the sensor is to be calibrated in the environment (where it will be established) in order to have *reference curves* for these three parameters then this set of information would determine the state of methanol in the environment, which could then be called the distinctive fingerprint of methanol.